International Journal of Electrical and Electronic Engineering & Telecommunications

ISSN 2319 – 2518 www.ijeetc.com
Vol. 1, No. 1, October 2012

Research Paper

IMPROVEMENT OF HYPERSPECTRAL IMAGE COMPRESSION AND DECOMPRESSION BASED ON WAVELET AND MODIFIED SPIHT IN MULTIMEDIA COMMUNICATIONS

S Vasuki[1]* and S Kala[2]

Corresponding Author: S Vasuki, ✉ hello_vasuki@yahoo.co.in

Satellites gather information from different sensors and send it using a temporal connection with very limited bandwidth. The bandwidth demand can be highly reduced, if the satellite preprocess the data and only sends relevant information. We focus on techniques that exploit spectral information exclusively to make decisions regarding the type of each-pixel-target or non target on a pixel-by-pixel basis in an image. Image data containing both spatial and spectral information and this information can be used to address such detection tasks. Image compression as one of the key enabling technologies in multimedia communications, which has been paid much attention in the past decades where the too key techniques like Discrete Wavelet Transforms (DWT) and Set Partitioning In Hierarchical Trees (SPIHT) have great influence on its final performance. Owe to the properties of fast computation, low memory requirement, DWT has been adopted as a new technical standard for still image compression. Further more, the traditional SPHIT algorithm has the drawbacks of long bits output and time consuming. In this paper, we propose a new technique named direction-adaptive lifting DWT. Then a modified SPHIT coding algorithm is present. It improves the scanning process and can effectively reduce the scaling bits length and running times.

Keywords: Discrete wavelet transforms, Set partition in hierarchical tree

INTRODUCTION

Hyperspectral imaging sensors provide image data containing both spatial and spectral information, and this information can be used to address such detection tasks. Hyperspectral imaging has been widely used in

[1] Department of Electronics and Communication, Velammal College of Engineering and Technology, Madurai (Dist), Viraganoor, Tamil Nadu, India.

[2] Department of Electronics and Communication, Sri Subramanya College of Engineering and Technology, Dindigul (Dist), Palani, Tamil Nadu, India.

remote sensing for the purposes such as resource management, agriculture, mineral exploration, and environmental monitoring. It uses an array of sensors to collect a set of images across the spectrum. The basic idea for hyper spectral imaging stems from the fact that, for any given material, the amount of radiation that is reflected, absorbed, or emitted—i.e., the radiance varies with wavelength. Hyperspectral imaging sensors measure the radiance of the materials within each pixel area at a very large number of contiguous spectral wavelength bands. A hyperspectral remote sensing system has four basic parts: the radiation (or illuminating) source, the atmospheric path, the imaged surface, and the sensor. In a passive remote sensing system the primary source of illumination is the sun. The distribution of the sun's emitted energy, as a function of wavelength throughout the electromagnetic spectrum, is known as the solar spectrum. The solar energy propagates through the atmosphere, and its intensity and spectral distributions are modified by the atmosphere as shown in Figure 1. The energy then interacts with the imaged surface materials and is reflected, transmitted, and/or absorbed by these materials. The reflected/emitted energy then passes back through the atmosphere, where it is subjected to additional intensity modifications and spectral changes. Finally, the energy reaches the sensor, where it is measured and converted into digital form for further processing and exploitation. The signal of interest, that is, the information bearing signal, is the reflectance spectrum defined by reflectance spectrum the energy. To understand hyper spectra ling data exploitation, it is important to realize how the presence of the atmosphere and the nature of the solar spectrum affect the relationship

Figure 1: Hyperspectral Imaging Sensors Measure the Spectral Radiance Information in a Scene to Detect Target Objects, Vehicles, and Camouflage in Open Areas, Shadows, and Tree Lines

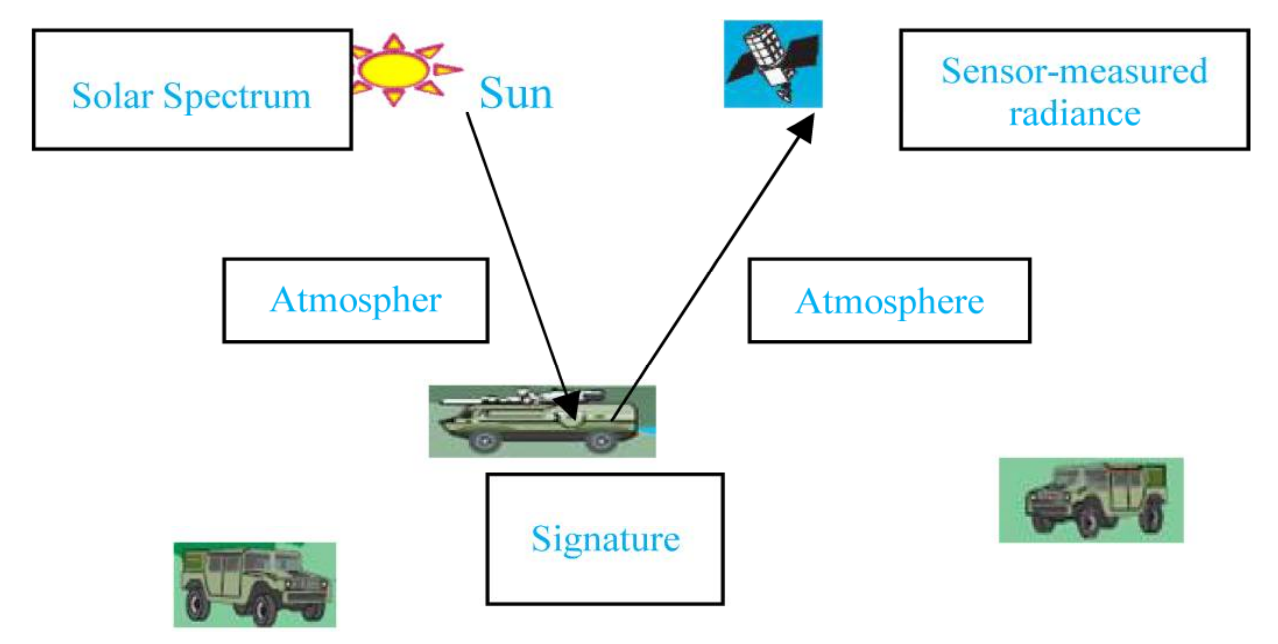

between the observed radiance spectra and the associated reflectance spectra. Basically, the observed spectrum would have the same shape as the reflectance spectrum if the solar spectrum were flat and the atmosphere had the same transmittance at all wavelengths. This unreasonably large dimension of hyperspectral images (HSIs) not only increases computational complexity but also degrades classification accuracy (Bioucas-Dias and Nascimento, 2008). Reduction of spectral dimensionality has been proven necessary to apply classification algorithms. Due to its simplicity and ease of use, the most popular Dimensionality Reduction (DR) approaches are Principal Component (PC) Analysis (PCA), Independent Component Analysis (ICA), Maximum Noise Fraction (MNF) and Discrete Wavelet Transform (DWT) (Chang and Du, 2004). However, those DR methods require a preliminary data arrangement. Indeed, when dealing with three-way data, a first step consists in vectorizing all images, yielding two way data, permitting the use of signal processing, but neglecting spatial rearrangement.

In the classical approach to hyper-spectral dimensionality reduction based on Principal Component Analysis (PCA), no meaning or behavior of the spectrum is considered and results are influenced by majority components in the scene. A spectral angle based classification before dimensionality reduction is a possible solution to this problem. Clustering based on support vectors using spectral based kernels is proposed in this work, which is found to generate good results in hyperspectral image classification. With Spectral Angle Mapping (SAM) is also done.

A hyperspectral image contains spatial domain and spectral domain components. The spectral vector represents the response of a sensor at various wavelengths and can be used to discriminate spectral features of minerals, soils, rocks, and vegetation (Motta *et al.*, 2006). Because of the large storage volume and spectral and spatial sample data redundancy, it is economical to compress hyperspectral images before transmitting them. The optical system divides the imaged ground area into a number of contiguous pixels. The ground area covered by each pixel (called the ground resolution cell) is determined by the Instantaneous Field Of View (IFOV) of the sensor system. The IFOV is a function of the optics of the sensor, the size of the detector elements, and the altitude.

EXISTING COMPRESSION METHODS

Basic compression methods for hyperspectral imagery are transform coding based algorithms (Chang and Du, 2004; and Zhang *et al.*, 2008), Vector Quantization (VQ) based algorithms (Penna *et al.*, 2007; and Akam *et al.*, 2010), Differential Pulse Code Modulation (DPCM) algorithm (Du and Fowler, 2007), and Adaptive Differential Pulse Code Modulation (ADPCM) (Baraniuk *et al.*, 2010). Conventionally, image decompression must be applied after compression. Some compression algorithms may increase the computational complexity. Few of them have been applied to image classification application. Signal-to Noise Ratio (SNR) is a popular measure of performance for these compression algorithms. However, high SNR is not necessary related to high classification accuracy.

The compression scheme consists of an image transform and a quantized. Computational cost can be saved since the proposed scheme does not require the inverse transform process. This scheme will be useful for those systems that need fast processing.

The classification error is fed back to the compression system and helps design the compression algorithm. With the help of the scheme in this paper, fewer operations are needed and the classification error can be obtained faster because the decompression step is eliminated. The main purpose of this paper is to show that it is possible to classify the transformed image. This hypothesis is based on our observation that classification on a radiance image and classification on a reflectance image yield very similar results.

The motivations of applying classification on a transformed image are that computational cost can be saved with fewer operations and classification accuracies of some classes with small subtle differences may be improved by enlarging these differences using a transform. In this paper, the Discrete Cosine Transform (DCT) is used for image transform, and a uniform quantize is applied after image transform.

Excessive data volume not only requires a large data depository system, but also requires a wider data transmission bandwidth between the satellite and the ground station. To mitigate the problem, state of the art data compression techniques are applied. Existing compression schemes such as JPEG are lossy and not efficient for the hyperspectral images because they fail to fully exploit the spectral data correlation.

The advent of the Discrete Wavelet Transform (DWT) and sub band-based decomposition systems in general (Baraniuk *et al.*, 2010), and their recognition as potential substitutes for the then ubiquitous Discrete Cosine Transform (DCT) (Cristophe *et al.*, 2008) led to the development of several compression systems.

Besides the algorithmic aspect, an efficient system implementation to support on-board processing, which alleviates the downlink bandwidth requirement, is crucial. Early attempt such as (Bioucas-Dias and Nascimento, 2008) adopted a Discrete Wavelet Transform (DWT) plus Set Partitioning In Hierarchical Trees (SPIHT) coding routine as the compression algorithm. The design was a stand-alone module and implemented in three Field-Programmable Gate Arrays (FPGAs). In Chang and Du (2004), a compression algorithm developed by NASA was implemented in a Xilinx FPGA platform equipped with an embedded PowerPC core. In Zhang *et al.* (2008), the compression algorithm was designed as a reconfigurable computing core and implemented in an FPGA with System-on-Chip (SoC) platform support. In Zhang *et al.* (2008), a “Fast Lossless” (FL) compression algorithm was implemented using FPGA. Due to the employment of a simple entropy coder facilitating a fully hardwired design, acceleration of 33 times faster than the software implementation was reported. In this letter, the emphasis will be on how to achieve a system implementation via Hardware/Software (HW/SW) codesign and on how to optimize the individual designs and minimize the HW/SW communication overhead.

The block diagram of the proposed lossless compression scheme, as shown in Figure 2, consists of three major modules, i.e., intraband prediction, interband prediction, and entropy coder. The intraband prediction is applied to the first image. The median predictor defined in JPEG-LS was employed due to its simplicity and efficiency. The interband prediction adopts a two-stage prediction approach and consists of three submodules. In initial prediction, a prediction reference value is first calculated. The multi-Look-Up Table (LUT) module uses it to look up the final prediction value. The quantized index module realizes a relaxation measure to reduce the lookup table sizes.

A look-up table indexed by the distinct pixel values in the previous band can be used store the corresponding pixel values in the current band to avoid the search effort. The table is updated constantly for each pixel prediction. Using multiple lookup tables can keep track of several latest mappings and yield better prediction results (Du and Fowler, 2007; Penna *et al.*, 2007; and Akam *et al.*, 2010). In our scheme, the number of LUT is set to five. To reduce the lookup table size, the table is indexed by a quantized instead of the original pixel value. The quantization factors are band independent and of the forms of power of two to avoid any division.

Figure 2: Block Diagram of Hyperspectral Image Compression Scheme

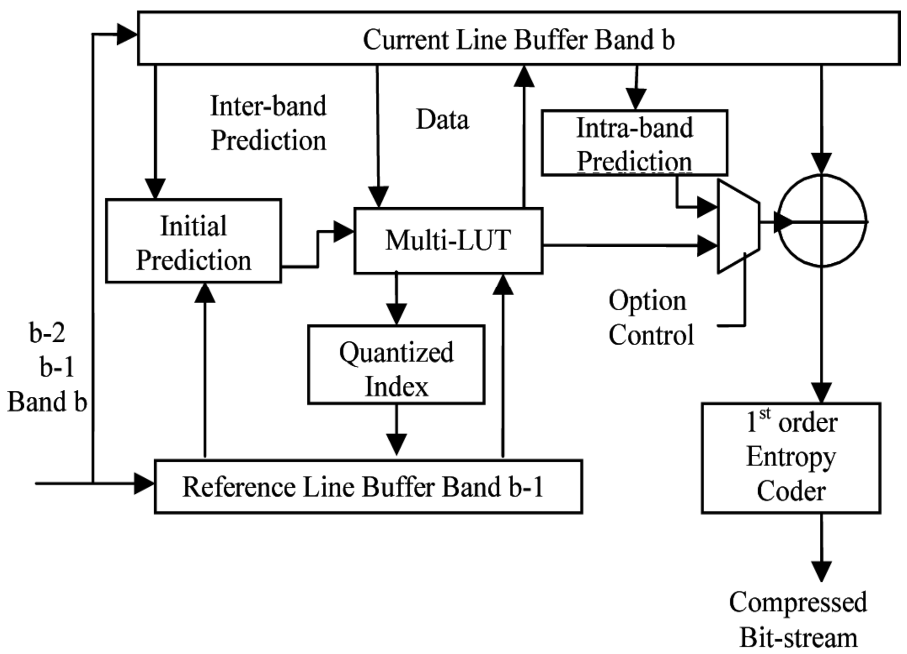

In entropy coding, the prediction errors are coded using separate entropy models for the sign bit and the magnitude. The sign bit model has three distinct symbols and the magnitude model contains 65 symbols. A first-order Adaptive Arithmetic Coding (AAC) scheme was used. Algorithm simulation results on the standard 1997 AVIRIS hyperspectral images indicate the proposed scheme can yield an average compression ratio of 3.74 and outperforms rival schemes (Du and Fowler, 2007; Penna *et al.*, 2007; and Akam *et al.*, 2010) by 4% to 12%.

DIRECTION-ADAPTIVE LIFTING DWT

In the images, different regions have different directions of the geometric characteristics of space, such as border or stripe. If all of the geometric characteristics of this geometry deal with the lifting with the same structure, it may ignore some features or cause larger error. Therefore, we focused on the geometric characteristics of the space relative to the most suitable direction of lifting.

By 1-D signal expect different definitions of the direction, here we only consider the horizontal structure.

In order to maintain the original space direction of the image characteristics, we still use the traditional split of lifting wavelet. 2-D signal $x(m, n)_{m, n \in Z}$ will be split into even $x_e(m, n) = x(m, 2n)$ and odd $x_o(m, n) = x(m, 2n + 1)$ set.

The prediction process, in Figure 3, assuming that the direction selected for the θ, and changing the original operator P into

$$P(x_e, m, n) = \Sigma \alpha_i x(m + \text{sign}(i - 1)\tan\theta, 2n + i) \quad ...(1)$$

Figure 3: Direction Predictor

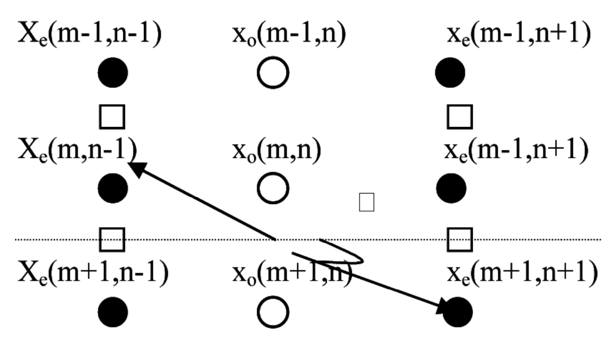

We can see that $m + \text{sign}(i - 1) \tan \theta$ is not always an integer from (1), i.e., there will be noninteger points. And these noninteger points do not exist in original image. This requires that we use the appropriate definition to give them values, and we call it as the process of interpolation. In the interpolation process, we limit the interpolation to the pixel which must be even set $x_e(m, n)$ in order to ensure perfect reconstruction. Interpolation through the following formula:

$$x(m + \text{sign}(i - 1)\tan \theta, 2n + i) = \Sigma \varphi_k x(m + k, 2n + i) \quad ...(2)$$

Where k represents point of $x(m + \text{sign}(i - 1) \tan \theta, 2n + i)$ in direction $\text{sign}(i - 1) \tan \theta$ and φ_k represents the interpolation coefficient. In this paper, Lagrange interpolation method is used to determine φ_k.

Similarly, during the update process operator U should be changed into

$$U(d, m, n) = \Sigma \beta_i d(m + \text{sign}(i)\tan \theta, 2n + i) \quad ...(3)$$

Since $m + \text{sign}(i - 1) \tan \theta$ is not always an integer, we can also use interpolation of the predicting process.

After above three steps, we can obtain a vertical high-pass sub band H and a low-pass sub band L, and then constitute in 2-D direction lifting structure by doing horizontal 1-D direction lifting.

The selection of the angle θ is the key. First, we choose the angle based on block, and the block size is 16×16. For each block, we select a pair of best directions of adaptive lifting (a vertical direction, a horizontal direction) to make the signal mostly smooth in this block. All pixels are lifting with the same direction in each block, and the direction of different block is to choose independently apart from the effects of other blocks. For an image, we need to select a pair of the best direction as lifting direction for each block. Finally, the entire image energy as much as possible concentrated in the low-frequency sub band (LL) after each block is lifted with their directions.

We first consider the choice of all the horizontal direction. We assume that the image I is cut into a series of 16 × 16 blocks, and denoted by

$$B_i,\ i = 1, 2, 3, ..., B_i) \cap B_j = \phi(i \neq j), \cup B_i = I$$

next, we assume that the θ is vertical direction of block B_i. We use the Rate-Distortion (RD) function to determine the best direction to lift for each block. First of all, we calculate the prediction error of the entire image as follows:

$$D(I) = \sum_{B_{i \in I}} \sum_{m,n} \left| dB_i, \theta(m, n) \right| \quad ...(4)$$

We can find that θ of B_i will independently impact the value of $D(I)$. $D(I)$ can be taken as a function of a series θ_1, θ_2, θ_3, ... If making $D(I)$ be the smallest value, block Bi must have the smallest error. Taking into account the coding of the direction of the various blocks needs additional information of bits, we adopt the following formula to determine the best direction to lifting as follows:

$$RD(\nabla) = D(I, \nabla) + \lambda R(\nabla), \nabla = \theta_{B1}, \theta_{B2}, \theta_{B3} \quad ...(5)$$

We set a threshold ä to decide $x_o(m, n)$ whether it is in a smooth or non smooth area after we obtain $P_1(x_o(m, n))$ and $P_2(x_o(m, n))$. That is, $x_o(m, n)$ is in the smooth area if $|P_1(x_o(m, n)) - P_2(x_o(m, n))| < \delta$ using the following formula to predict:

$$P_1(x_o(m, n)) = \sum_{i=-K+1,\, i \neq 0}^{K} \frac{\prod_{j \neq i} x\left(m + sign(i-1)\tan\theta,\ 2n + i\right)\left(m - m_i\right)}{\prod_{j \neq i}\left(m_i - m_j\right)} \quad ...(6)$$

On the contrary, $x_o(m, n)$ is in a non smooth area and then reconsider its forecast for selection of side of the pixels associated with higher value. Taking off the pixel of other sides, we only consider one side to predict $x_o(m, n)$ again, and will obtain two new predicted values $P_3(x_o(m, n))$ and $P_4(x_o(m, n))$. In order to perfect reconstruction $x_o(m, n)$, we cannot directly compare these two predicted values with $x_o(m, n)$, instead, we compare two values which are most close values to $x_o(m, n)$, $x_e(m + 1, n - \tan\theta)$ with $x_e(m, n + \tan\theta)$ as follows:

$$\delta_1 = |x_e(m, n + \tan\theta) - P_3(x_o(m, n))| \quad ...(7)$$

$$\delta_2 = |x_e(m + 1, n - \tan\theta) - P_4(x_o(m, n))| \quad ...(8)$$

Comprising δ_1 with δ_2, we obtain predict operator by using more correlation side as follows:

$$P(x_o(m, n)) = P_3(x_o(m, n))\delta_1 < \delta_2$$

$$P(x_o(m, n)) = P_4(x_o(m, n))\delta_1 > \delta_2 \quad ...(9)$$

MODIFIED SPIHT ALGORITHM

Image compression plays a major role in multimedia applications. Many powerful and complex wavelet-based image compression schemes have been developed over the past few years. Among them, SPIHT is the well recognized coding method because of its excellent RD performance. However, it does not entirely provide the desired features of progressive transmission and spatial scalability due to the algorithm uses an

Figure 4: First Level of Wavelet Transform Decomposition of Barbara

(a) 5/3 Wavelet

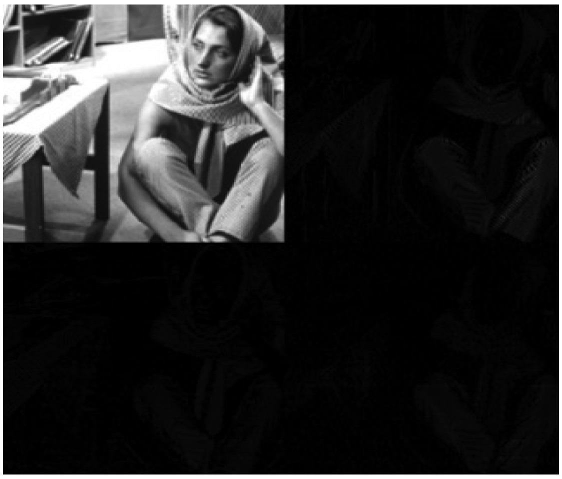

(b) Directional Aadaptive

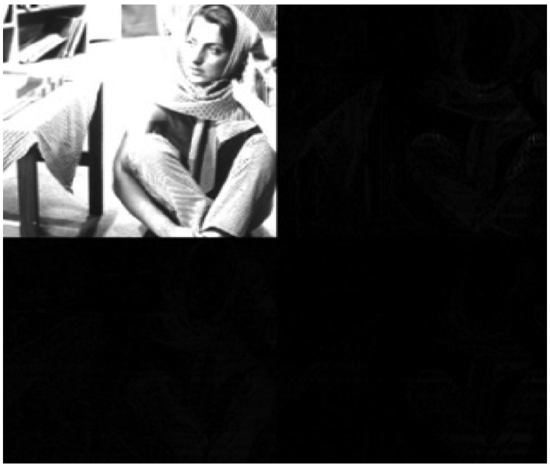

(c) Interpolation

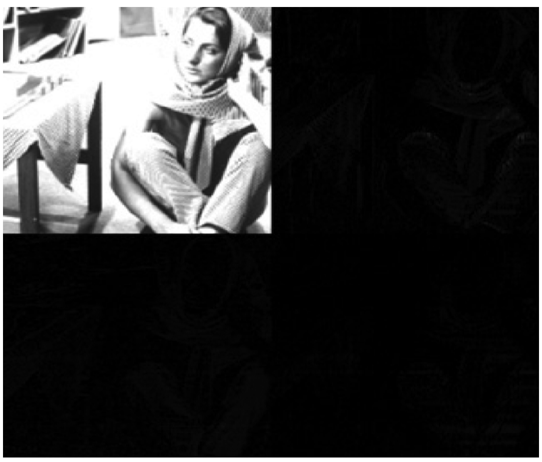

inefficient coefficient partitioning method. Moreover, a larger amount of memory is required to maintain three lists that are used for storing the coordinates of the coefficients and tree sets in the coding and decoding process. A great number of operations to manipulate the memory are also required in the codec scheme, which greatly reduces the speed of the coding procedure.

In this paper, we propose a modified SPIHT coding algorithm, which can reduce bits redundancy and scanning redundancy of traditional SPIHT. When scanning the collection of type-D in List of Insignificant Sets (LIS), if there are important coefficients in their offspring, traditional SPIHT will generate three direct child nodes of their offspring and determine the importance of child nodes to decide where to send these child nodes, list of significant pixels or list of insignificant pixels, and meanwhile it generates a L-type set to LIS. However, the probability of important coefficients being a direct descendant is not very high in practice, especially for complex image textures. Therefore, we should deal with $O(i, j)$ as a whole, and then determine the importance of the coefficients to decide whether or not to split the collection.

Traditional SPIHT always outputs 4 bits to determine the importance of child nodes. If the child node is not an important coefficient, we can reduce the output to 1 bit by using our method. Experimental results show that our method can reduce the SPIHT encoding bits of the reconstructed stream.

Here, we present the modified SPIHT algorithm with two improvements. When the threshold is too large or too small, $O(i, j)$ will be not so important. Through lots of experiments, we find that when the threshold value is less than 4, $O(i, j)$ is almost not used. Therefore, when the threshold is equal to or greater than 4, we improve the ratio of important coefficients in the bit-stream. While the threshold is smaller, then we use the traditional SPIHT. When scanning a large threshold, the generated $O(i, j)$ replaces the four children nodes of following scan, and it lasts lots of the threshold scan level. Therefore, you can save more bits.

EXPERIMENTAL RESULTS AND ANALYSIS

In this part, we first compare the performance of interpolation-based method with the non interpolation one. After that the performance of modified SPIHT is tested. Finally, we compare the performance of our methods with the traditional methods.

Experiment 1: Performance of DWT Algorithm

We perform wavelet decomposition to Barbara, which has obvious characteristics of local spatial geometry to do comparison. As can be seen from Figure 4, the directional adaptive wavelet has much smaller high-frequency sub band coefficients than 5/3 wavelet in the low-frequency images, using the interpolation-based method that retains most of the details of the information than non striped area. The textures of shelves, pants, and striped wallpaper are more apparent.

Each sub band energy percentage of the whole image. We can see energy is more concentrated by using the interpolation-based directional-adaptive lifting wavelet, so that subsequent coding process in image compression can be more effective.

Experiment 2: Performance of SPIHT Algorithm

The modified SPIHT algorithm does not use any point interception stream approach, and the interception approach using quantitative threshold decision method, means that each time quantitative threshold scan must be completed. After the scanning is completed, determination will be taken on the resulting stream to decide whether to continue scanning the next level of quantization threshold scan.

So with this implementation, at the same compression ratio (compression ratio can be considered as a bandwidth limit here), the modified SPIHT and the traditional SPIHT method both have the same Peak Signal-to-Noise Ratio (PSNR) after the reconstruction of generated code stream to the image; this is because the modified method of this paper is to quantify the current threshold for scanning all of the important factors, the effect is the same as the traditional SPIHT. Therefore, in the corresponding position, at each level of the reconstructed quantization threshold coefficient is same. Although PSNR is same, in the same bandwidth, the number of bits that are generated by the modified SPIHT algorithm are less than the traditional SPIHT, so the operation is more efficient.

CONCLUSION

Image compression is one of the key-enabling technologies in multimedia communications, especially DWT and SPIHT are widely used. This paper focused on the lifting wavelet image coding compression. Our work mainly focused on the following aspects.

1. This paper first proposed a new kind of lifting wavelet structure, which combined with Lagrange interpolation method.

2. The proposed method can make an adaptive selection of best lifting direction, and use Lagrange interpolation to predict according to local characteristics between the pixels. Experimental results showed that the method has more advantages than the conventional lifting scheme.

3. After that, the paper presented a modified SPIHT algorithm. The algorithm reduced bits redundant and scanning redundancy of traditional SPIHT. Experimental results proved that the algorithm can reduce the number of bits and runtime effectively without compromising coding quality.

   The future works are as follows.

- Although the PSNR has increased, the proposed lifting wavelet structure costs a significant amount of time when it makes the adaptive directional choice because of considering the RD of each angle. This needs to be solved in the future work.
- While at the same PSNR, the modified SPIHT coding algorithm can reduce the number of bits. But in this paper, we cannot realize interception capabilities of any point. It also needs to be considered in future work.

The results of this work demonstrated that bit rate allocation based on the image content of the individual spectral bands has a significant impact on decompressed image quality. As electronic components such as memories and FPGAs become smaller, more compression functionality and more complex bit rate allocation algorithms can be placed in smaller and faster systems.

REFERENCES

1. Akam Bita I P, Barret M and Pham D-T (2010), "On Optimal Transforms in Lossy Compression of Multicomponent Images with JPEG2000", *Signal Process*, Vol. 90, No. 3, pp. 759-773.
2. Baraniuk R G, Cevher V, Duarte M F and Hegde C (2010), "Model-Based Compressive Sensing", *IEEE Trans. Inf. Theory*, Vol. 56, No. 4, pp. 1982-2001.
3. Bioucas-Dias J and Nascimento J (2008), "Hyperspectral Subspace Identification", *IEEE Trans. Geosci. Remote Sens.*, Vol. 46, No. 8, pp. 2435-2445.
4. Chang C-I and Du Q (2004), "Estimation of Number of Spectrally Distinct Signal Sources in Hyperspectral Imagery", *IEEE Trans. Geosci. Remote Sens.*, Vol. 42, No. 3, pp. 608-619.
5. Cristophe E, Mailhes C and Duhamel P (2008), "Hyperspectral Image Compression: Adapting SPIHT and EZW to Nisotropic 3-D Wavelet Coding", *IEEE Trans. Image Proc.*, Vol. 17, No. 12, pp. 2334-2346.
6. Du Q and Fowler J E (2007), "Hyperspectral Image Compression Using JPEG2000 and Principal Component Analysis", *IEEE Geosci. Remote Sens. Lett.*, Vol. 4, No. 2, pp. 201-205.
7. Motta F Rizzo and Storer J A (Eds.) (2006), "Hyperspectral Data Compression", Springer-Verlag, Berlin, Germany.
8. Penna B, Tillo T, Magli E and Olmo G (2007), "Transform Coding Techniques for

Lossy Hyperspectral Data Compression”, *IEEE Trans. Geosci. Remote Sens.*, Vol. 45, No. 5, pp. 1408-1421.

9. Zhang J, Fowler J E and Liu G (2008), “Lossy-to-Lossless Compression of Hyperspectral Imagery Using Three-Dimensional TCE and an Integer KLT”, *IEEE Geosci. Remote Sens. Lett.*, Vol. 5, No. 4, pp. 814-818.